



**HAL**  
open science

## Photodegradation of novel oral anticoagulants under sunlight irradiation in aqueous matrices

Montaha Yassine, Laura Fuster, Marie-Hélène Devier, Emmanuel Geneste, Patrick Pardon, Axelle Grelard, Erick Dufourc, Mohamad Al Iskandarani, Selim Ait-Aissa, Jeanne Garric, et al.

### ► To cite this version:

Montaha Yassine, Laura Fuster, Marie-Hélène Devier, Emmanuel Geneste, Patrick Pardon, et al.. Photodegradation of novel oral anticoagulants under sunlight irradiation in aqueous matrices. *Chemosphere*, 2018, 193, pp.329-336. 10.1016/j.chemosphere.2017.11.036 . ineris-01863205

**HAL Id: ineris-01863205**

**<https://ineris.hal.science/ineris-01863205>**

Submitted on 28 Aug 2018

**HAL** is a multi-disciplinary open access archive for the deposit and dissemination of scientific research documents, whether they are published or not. The documents may come from teaching and research institutions in France or abroad, or from public or private research centers.

L'archive ouverte pluridisciplinaire **HAL**, est destinée au dépôt et à la diffusion de documents scientifiques de niveau recherche, publiés ou non, émanant des établissements d'enseignement et de recherche français ou étrangers, des laboratoires publics ou privés.

1 Photodegradation of novel oral anticoagulants under sunlight irradiation in  
2 aqueous matrices

3  
4 Montaha Yassine<sup>1ab,2</sup>, Laura Fuster<sup>1ab</sup>, Marie-Hélène Dévier<sup>1ab</sup>, Emmanuel Geneste<sup>1ab</sup>, Patrick  
5 Pardon<sup>1ab</sup>, Axelle Grélard<sup>3</sup>, Erick Dufourc<sup>3</sup>, Mohamad Al Iskandarani<sup>2</sup>, Selim Aït-Aïssa<sup>4</sup>,  
6 Jeanne Garric<sup>5</sup>, Hélène Budzinski<sup>1ab</sup>, Patrick Mazellier<sup>1ab</sup>, Aurélien S. Trivella<sup>1ab,\*</sup>

7  
8 <sup>1a</sup>Univ. Bordeaux, UMR EPOC CNRS 5805, LPTC, F-33405 Talence, France

9 <sup>1b</sup>CNRS, EPOC, UMR 5805, LPTC, F-33400 Talence, France

10 <sup>2</sup>National Council of Scientific Research (NCSR), Lebanese Atomic Energy Commission  
11 (LAEC), Laboratory of Analysis of Organic Pollutants (LAOP), B. P. 11-8281, Riad El Solh -  
12 1107 2260 - Beirut, Lebanon

13 <sup>3</sup>Institute of Chemistry and Biology of Membranes and Nano-objects, CBMN UMR 5248,  
14 CNRS University of Bordeaux, Bordeaux National Institute of Technology, Allée Geoffroy St  
15 Hilaire, Pessac, France

16 <sup>4</sup>INERIS, Unité d'écotoxicologie *in vitro* et *in vivo* (ECOT), Verneuil-en-Halatte, France

17 <sup>5</sup>Irstea, UR MALY, centre de Lyon-Villeurbanne, F-69616 Villeurbanne, France

18  
19  
20 \*Corresponding author: Aurélien Trivella

21 [aurelien.trivella@u-bordeaux.fr](mailto:aurelien.trivella@u-bordeaux.fr)

22 Tel: +33 (0)553352429

23

24

25 **Abstract**

26 Kinetics of photodegradation of novel oral anticoagulants dabigatran, rivaroxaban, and  
27 apixaban were studied under simulated solar light irradiation in purified, mineral, and river  
28 waters. Dabigatran and rivaroxaban underwent direct photolysis with polychromatic quantum  
29 yields of  $2.2 \times 10^{-4}$  and  $4.4 \times 10^{-2}$ , respectively. The direct photodegradation of apixaban was not  
30 observed after 19 hours of irradiation. Kinetics of degradation of rivaroxaban was not  
31 impacted by the nature of the aqueous matrix while photosensitization from nitrate ions was  
32 observed for dabigatran and apixaban dissolved in a mineral water. The photosensitized  
33 reactions were limited in the tested river water (Isle River, Périgueux, France) certainly due to  
34 the hydroxyl radical scavenging effect of the dissolved organic matter. The study of  
35 photoproduct structures allowed to identify two compounds for dabigatran. One of them is the  
36 4-aminobenzamidine while the second one is a cyclisation product. In the case of rivaroxaban,  
37 as studied by very high field NMR, only one photoproduct was observed *i.e.* a photoisomer.  
38 Finally, seven photoproducts were clearly identified from the degradation of apixaban under  
39 simulated solar light.

40

41 **Keywords:** photolysis; solar light irradiation; surface water; apixaban; dabigatran;

42 rivaroxaban

43

44

## 45 **1. Introduction**

46 Until recently, oral anticoagulants were synonyms of vitamin K antagonists (VKAs) such as  
47 warfarin. These medicines are used for venous thromboembolism, stroke, atrial fibrillation  
48 treatment, and most generally in medicinal conditions that require chronic anticoagulation  
49 (Hanslik et al., 2004). VKAs may not be appropriate for many patients especially due to the  
50 necessity of dietary precautions and frequent laboratory monitoring (El-Helou et al., 2013). In  
51 fact, if warfarin concentration is too low the anticoagulation effect does not act efficiently; a  
52 too high concentration causes excessive bleeding. In this context, novel oral anticoagulants  
53 (NOACs) were developed (Spyropoulos, 2008; Beyer-Westendorf et al., 2014). The U.S.  
54 Food and Drug Administration (F.D.A.) recently approved the use of three new active  
55 ingredients, namely dabigatran etexilate (2010), rivaroxaban (2011), and apixaban (2012)  
56 (Wanat, 2013). Dabigatran etexilate is a prodrug that is converted to dabigatran and acts as a  
57 direct thrombin inhibitor (Khoo et al., 2010). Rivaroxaban and apixaban are direct factor Xa  
58 inhibitors that do not require cofactors for activity (Gulseth et al., 2008; Frost et al., 2013).  
59 These three compounds are also increasingly used in Europe. In particular, these NOACs  
60 currently represent 30% of ingested anticoagulants in France with an increase in their  
61 consumption by a factor of 10 between the second trimester 2012 and the third trimester 2013  
62 (ANSM, 2013). The main limitation for their use was the absence of antidote. In 2015, the  
63 F.D.A. approved the idarucizumab as dabigatran antidote while rivaroxaban and apixaban  
64 antidote (andexanet alpha) is about to be validated (Pollack et al., 2015; Siegal et al., 2015).  
65 Thus, their prescriptions are expected to continue to rise in the near future.

66 To our knowledge, information reported in the literature about the occurrence of NOACs in  
67 the aquatic compartment, their fates, and their toxicity, as well as their degradation products  
68 are very scarce (Kasad, 2013; Ramiseti et al., 2014; Secrétan et al., 2015; Swain et al., 2016;  
69 Tantawy et al., 2016; Wingert et al., 2016). This is especially worrying since human

70 metabolism studies have shown that NOACs are eliminated in urines as unchanged forms at  
71 levels between 27 and 85% of the delivered dose (eVidal, 2017). In fact, organic pollutants  
72 are known to undergo degradation processes in environmental waters which must be taken  
73 into consideration. Photolysis can be one of the major ways of degradation for pharmaceutical  
74 compounds absorbing solar light as well as for those degraded by photosensitization (Szabo et  
75 al., 2011; Zuo et al., 2013; Carlson et al., 2015; Zhang et al., 2016; Chen et al., 2017).  
76 This study has for objective to bring information on the environmental fate of NOACs. In  
77 particular, direct and indirect photolysis of NOACs was studied in different aqueous matrices.  
78 Results on molar absorption coefficients, rate constants and polychromatic quantum yields of  
79 photodegradation are discussed. Rate constants were obtained from simulated solar light  
80 irradiation in purified, mineral, and river waters to evaluate the effect of ions and dissolved  
81 organic matter naturally present in surface waters. Finally, the elucidation of structures of  
82 photoproducts was performed using LC-HRMS, and 700 and 800 MHz NMR spectrometers.  
83

## 84 2. Materials and methods

85 **2.1. Chemicals.** The novel oral anticoagulants (NOACs) dabigatran (APIChem Technology,  
86 CAS 211914-51-1, 99%), rivaroxaban (AKSci, CAS 366789-02-8, 98%), and apixaban  
87 (APIChem Technology, CAS 503612-47-3, 99%), as well as 4-aminobenzamidine  
88 dihydrochloride ( $\geq 99.0\%$ ), methanol (CHROMASOLV®,  $\geq 99.9\%$ ), and sodium bicarbonate  
89 salt ( $\geq 99.5\%$ ) were purchased from Sigma-Aldrich (Saint-Quentin Fallavier, France). Sodium  
90 nitrate salt (analytical reagent grade) was provided by Fisher Chemical. All chemicals were  
91 used as received. Purified water was produced using a Milli-Q® Direct-Q® 5 system  
92 (Millipore, resistivity 18.2 M $\Omega$ .cm). Mineral water (Volvic) contains 7.2 and 74.0 mg.L<sup>-1</sup> of  
93 nitrate and hydrogen carbonate ions, respectively. River water was collected from the Isle  
94 River (Périgueux, France). This surface water contained 7.7 and 140-200 mg.L<sup>-1</sup> of nitrate and  
95 hydrogen carbonate ions, respectively. Before use, the river water was filtered on a 0.45  $\mu$ m  
96 hydrophilic PVDF Durapore® membrane (Millipore). Stock solutions of NOACs were  
97 prepared in purified water at concentrations of  $5.0 \times 10^{-5}$ ,  $1.0 \times 10^{-5}$ , and  $3.0 \times 10^{-6}$  mol.L<sup>-1</sup> for  
98 dabigatran, rivaroxaban, and apixaban, respectively. During the preparation, volumetric flasks  
99 were covered with aluminum foils and solutions were left under magnetic stirring during one  
100 week. Then, stock solutions were stored in amber glass bottles at room temperature until use  
101 to prevent photodegradation and solubility problems, respectively. The stability of the three  
102 compounds was checked.

103

104 **2.2. UV-Visible spectroscopy.** UV-Visible absorption spectra were recorded on a UV-1800  
105 spectrophotometer (Shimadzu, Japan). A 1-nm resolution and a “medium” scan rate were  
106 used to record the reference spectrum and spectra in the range 200-400 nm (NOACs do not  
107 absorb visible light) using either 1 or 5 cm quartz cells (QS, Hellma Analytics).

108 Molar absorption coefficients of dabigatran and rivaroxaban in purified water were calculated  
109 from the absorbance of five solutions with concentrations included in the range  $10^{-6}$  -  $10^{-5}$   
110 mol.L<sup>-1</sup>. Due to the particularly low solubility of apixaban in water, a stock solution was  
111 prepared in methanol at a concentration of  $9.6 \times 10^{-6}$  mol.L<sup>-1</sup>. Then, this stock solution was  
112 used to prepare five solutions at concentrations between  $1.0 \times 10^{-6}$  and  $4.8 \times 10^{-6}$  mol.L<sup>-1</sup> by  
113 adding purified water (*i.e.* the maximal proportion of methanol was of 50%).  
114 The solar light emission spectrum at the Earth surface was recorded using a USB2000+  
115 radiometer coupled to an optical fiber (Ocean Optics, Florida, USA).

116  
117 **2.3. Irradiation experiments.** Solar radiations at the Earth surface were simulated using a  
118 SUNTEST CPS apparatus from Atlas Material Testing Solutions (Illinois, USA). The  
119 irradiance was set to 250 W.m<sup>2</sup>. In the case of kinetic studies, purified, mineral, and river  
120 waters were spiked with the stock solutions prepared in purified water to obtain final  
121 concentrations of  $3.5 \times 10^{-7}$ ,  $3.5 \times 10^{-7}$ , and  $4.5 \times 10^{-7}$  mol.L<sup>-1</sup> for dabigatran, rivaroxaban, and  
122 apixaban, respectively. For the elucidation of photoproduct structures, non-irradiated and  
123 irradiated stock solutions were analyzed without pre-treatment.

124 Before irradiation, samples were placed into 12 mL transparent glass tubes (optical  
125 pathlength: 1.5 cm) and were sealed to avoid water evaporation. NOACs were irradiated in  
126 purified water alone and doped with nitrate and bicarbonate ions (same concentrations as in  
127 mineral water), in mineral water, and in river water. For each aqueous matrix, two tubes were  
128 filled with 10 mL of solution and one of them was wrapped in an aluminum foil for dark  
129 control. To obtain kinetic data, aliquots of each sample were collected before irradiation and  
130 after scheduled irradiation time. For each kinetics, at least five samplings were performed and  
131 the analysis was repeated in triplicate. The maximum irradiation time was of 10 hours for  
132 dabigatran, 4 hours for rivaroxaban, and 19 hours for apixaban. To calculate the

133 polychromatic quantum yields of photodegradation, photon fluence rates were measured with  
134 a one nanometer interval in the range 290-350 nm using a USB2000+ radiometer coupled to  
135 an optical fiber (Ocean Optics, Florida, USA).

136

137 **2.4. HPLC and LC-QToF-MS analyses.** For kinetics studies, HPLC analyses were carried  
138 out using an Agilent 1100 series chromatograph (Agilent Technologies) equipped with a  
139 variable wavelength detector (Zuo, 2014). For dabigatran and rivaroxaban, the column was a  
140 Nucleosil® C<sub>18</sub> Nautilus, 250 mm x 4.6 mm, with a particle size of 5 µm (Macherey-Nagel)  
141 while for apixaban the column was a Nucleodur® 100-5 C<sub>18</sub> ec, 250 mm x 4.6 mm, with a  
142 particle size of 5 µm (Macherey-Nagel). Solvent A was methanol and solvent B purified  
143 water. Analyses were carried out in isocratic mode with a ratio of 60:40 (A:B, v/v) for  
144 rivaroxaban and apixaban, and a ratio of 30:70 (A:B, v/v) for dabigatran. The UV detection  
145 was performed at 303, 248, and 277 nm for dabigatran, rivaroxaban, and apixaban,  
146 respectively.

147 UV absorption spectra of photoproducts were recorded with an HPLC Spectra System P1000  
148 coupled with a diode array detector model UV6000LP (Thermo Separation® Products). For  
149 each NOAC, elution conditions described above were used. With the goal to check the elution  
150 of all the products formed after irradiation, other analyses were performed in gradient mode.  
151 The gradient elution started with 10% of A and reached 100% in 25 minutes linearly. Then, it  
152 was kept stable during 5 minutes. No new photoproducts were observed compared to isocratic  
153 mode analyses.

154 LC-HRMS analyses were carried out using an Agilent 1290 HPLC system coupled to an  
155 Agilent 6540 QToF mass spectrometer (Agilent Technologies, Inc., Santa Clara, CA, USA)  
156 equipped with an Agilent Jet Stream electrospray ionization source (ESI). The  
157 chromatographic separation of the parent compound and of its photoproducts was performed

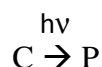


158 on a Kinetex C<sub>18</sub> column (100 x 2.1 mm, 1.7 μm; Phenomenex®, Agilent Technologies, Les  
159 Ulis, France ) regulated at 40°C. Gradient LC elution was performed at a flow rate of 0.3  
160 mL.min<sup>-1</sup> using 0.1% formic acid in purified water as mobile phase A and 0.1% formic acid in  
161 acetonitrile as mobile phase B. The gradient started with 10% of B and was linearly increased  
162 to 35% in 13 minutes. The fraction B was then immediately increased and held at 100% for 1  
163 min, before returning to the starting conditions for 3 min. Sample injection volume was set at  
164 5 μL. Non-irradiated and irradiated stock solutions in purified water were analyzed without  
165 pre-treatment.

166 After elution, the analytes were detected using the QToF operating in positive ion mode  
167 (ESI+) with the following parameters: capillary voltage, 3000 V; nebulizer pressure, 40 psig;  
168 drying gas, 8 L/min; gas temperature, 300 °C; sheath gas flow, 11 L/min; sheath gas  
169 temperature, 400 C; nozzle voltage, 0 V; fragmentor voltage, 190 V. LC-MS accurate mass  
170 spectra were recorded across the range m/z 70 – 1000 at 2 GHz. The data recorded were  
171 processed with MassHunter Qualitative software (version B.06.00, Agilent Technologies,  
172 Santa Clara, CA, USA). Accurate mass measurements of each peak from the extracted ion  
173 chromatograms were obtained by means of a calibrant solution delivered by an external  
174 quaternary pump, allowing system to continuously correct for any mass drift by using the  
175 reference mass ion HP-921 [hexakis-(1H,1H,3H-tetrafluoropropoxy)-phosphazine] at m/z  
176 922.0098. Stability of mass accuracy was checked before, and if values went above 0.2 ppm  
177 error, then the instrument was recalibrated. The instrument was operated in single MS with  
178 full spectra (1 spectrum/s) and in MS/MS (2 spectra/s) using an isolation width set at medium  
179 (m/z ~ 4), and collision energies of 10, 20, and 40 eV. A standard solution containing 36  
180 compounds was injected before the samples to check the retention time of compounds and the  
181 instrumental sensitivity.

182

183 **2.5. Rate constants and polychromatic quantum yields.** Following the absorption of a  
 184 photon, an organic contaminant (C) can be degraded and one or several photoproducts (P) are  
 185 formed. The equation of the reaction is:



187 Under specific experimental conditions (*i.e.* low absorbance), this reaction generally follows  
 188 an apparent first-order kinetics modeled by equation 1:

$$189 \quad \ln\left(\frac{[C]_0}{[C]_t}\right) = k_{poly} \cdot t \quad \text{eq. (1)}$$

190 where  $[C]_0$  and  $[C]_t$  are the organic contaminant concentrations ( $\text{mol.L}^{-1}$ ) respectively before  
 191 irradiation and at the instant  $t$ ,  $k_{poly}$  is the apparent first-order rate constant under  
 192 polychromatic irradiation ( $\text{s}^{-1}$ ), and  $t$  is the irradiation time (s).

193 In this framework, the rate of photolysis of C is given by equation 2:

$$194 \quad v(C) = k_{poly} \cdot [C]_t = \sum_{\lambda_1}^{\lambda_n} I_{0,\lambda_i} \cdot (1 - e^{-2.303 \cdot A_{\lambda_i}}) \cdot \phi_{\lambda_i} \quad \text{eq. (2)}$$

195 where  $I_{0,\lambda_i}$  is the photon fluence rate of the irradiation source ( $\text{E.L}^{-1} \cdot \text{s}^{-1}$ ),  $A_{\lambda_i}$  is the absorbance  
 196 of C and  $\phi_{\lambda_i}$  is the quantum yield of photolysis of C ( $\text{mol.E}^{-1}$ ) at the  $\lambda_i$  wavelength.  $\lambda_1$ - $\lambda_n$  is  
 197 the overlapping wavelength range between the UV-Vis absorptions of the organic  
 198 contaminant and the emission spectrum of the radiation source.

199 In environmental conditions, the absorbance of C is generally low ( $A < 0.02$ , hyper dilute  
 200 medium). Based on this hypothesis, the expression of polychromatic quantum yield of  
 201 photolysis ( $\phi_{poly}$ ,  $\text{mol.E}^{-1}$ ) of C is given by equation 3:

$$202 \quad \phi_{poly} = \frac{k_{poly}}{2.303 \cdot l} \cdot \sum_{\lambda_1}^{\lambda_n} \frac{1}{\varepsilon_{\lambda_i} \cdot I_{0,\lambda_i}} \quad \text{eq. (3)}$$

203 where  $l$  is the sample's optical pathlength (cm) and  $\varepsilon_{\lambda_i}$  is the molar absorption coefficient  
 204 ( $\text{L.mol}^{-1} \cdot \text{cm}^{-1}$ ) at the  $\lambda_i$  wavelength.

205

206 **2.6. Nuclear magnetic resonance spectroscopy.** LC-QToF-MS analyses were not enough to  
207 identify the structure of the rivaroxaban photoproduct due to the same fragmentation pattern  
208 (see supplementary materials). The main limitation for NMR analyses was the low solubility  
209 of rivaroxaban in water and thus the low concentration of its degradation product. In order to  
210 concentrate both compounds, a solution of rivaroxaban was prepared in methanol at an initial  
211 concentration of  $52.9 \text{ mg.L}^{-1}$  and was irradiated with a SUNTEST CPS+ ( $250 \text{ W.m}^{-2}$ ) during 8  
212 hours. A volume of 8 mL of this solution was evaporated and the residue dissolved in 500  $\mu\text{L}$   
213 of methanol- $\text{d}_3$  (Eurisotop, France) for NMR experiments. The photochemical reactivity of  
214 rivaroxaban was the same in purified water and in methanol. A second sample of pure  
215 rivaroxaban (few mg of powder were dissolved in methanol- $\text{d}_3$ ) was prepared.  
216 1D and 2D NMR spectra of non-irradiated and irradiated rivaroxaban were recorded at room  
217 temperature on Bruker Avance III HD SB 700 MHz and 800 MHz spectrometers. The 700  
218 MHz spectrometer was equipped with a 5 mm  $^1\text{H}$ - $^{13}\text{C}$ / $^{15}\text{N}$ /D TXI probe with Z-gradients  
219 operating at 176.07 MHz and 700.15 MHz for  $^{13}\text{C}$  and  $^1\text{H}$ , respectively. The 800 MHz  
220 spectrometer was equipped with a 5 mm  $^1\text{H}$ - $^{13}\text{C}$ / $^{15}\text{N}$ /D TCI cryoprobe with Z-gradients  
221 operating at 81,08 MHz, 201.21 MHz and 800.23 MHz for  $^{15}\text{N}$ ,  $^{13}\text{C}$  and  $^1\text{H}$ , respectively. In  
222 order to assign the 2 structures, the following experiments were performed: 1D- $^1\text{H}$  and 1D-  
223  $^{13}\text{C}$  experiments and, HSQC  $^1\text{H}$ - $^{13}\text{C}$ , HMBC  $^1\text{H}$ - $^{13}\text{C}$ , COSY, TOCSY, NOESY, and SOFAST-  
224 HMQC  $^1\text{H}$ - $^{15}\text{N}$ , two-dimensional experiments. Data treatment was accomplished using the  
225 TopSpin Bruker software.

226

227

### 228 3. Results and discussion

229 **3.1. Ultraviolet absorption spectra.** UV absorption spectra of dabigatran, rivaroxaban, and  
230 apixaban, are presented in Fig. 1. Dabigatran dissolved in deionized water displays two  
231 maxima located at 302 nm ( $\epsilon_{302} = 24\,180\text{ L}\cdot\text{mol}^{-1}\cdot\text{cm}^{-1}$ ) and 220 nm ( $\epsilon_{220} = 40\,940\text{ L}\cdot\text{mol}^{-1}\cdot\text{cm}^{-1}$ ).  
232 In the case of rivaroxaban, the spectrum recorded in the aqueous medium shows a  
233 maximum at 248 nm ( $\epsilon = 23\,820\text{ L}\cdot\text{mol}^{-1}\cdot\text{cm}^{-1}$ ). Moreover, a shoulder was observed at 273 nm  
234 ( $\epsilon = 14\,930\text{ L}\cdot\text{mol}^{-1}\cdot\text{cm}^{-1}$ ). UV absorptions of apixaban have been studied in a mixture of  
235 methanol and water due to the very low solubility of the drug into the aqueous solvent. A  
236 maximum of absorption is observed at 278 nm ( $\epsilon = 14\,320\text{ L}\cdot\text{mol}^{-1}\cdot\text{cm}^{-1}$ ). This maximum was  
237 found at the same wavelength in pure methanol ( $9.6\times 10^{-6}\text{ mol}\cdot\text{L}^{-1}$ ) and in pure water ( $3.0\times 10^{-6}$   
238  $\text{mol}\cdot\text{L}^{-1}$ ). The calculated molar absorption coefficient in pure methanol was of  $14\,700\text{ L}\cdot\text{mol}^{-1}\cdot\text{cm}^{-1}$ .  
239

240  
241 **Please insert Fig. 1.**

242  
243 The three novel oral anticoagulants (NOACs) absorb photons above 300 nm. Therefore, they  
244 absorb the solar light reaching the Earth surface and they can undergo direct photolysis (Fig.  
245 1). The study of this abiotic degradation pathway is of main concern from the environmental  
246 point of view. Moreover, the role of ions and dissolved organic matter (DOM) naturally  
247 present in surface waters is also discussed further.

248  
249 **3.2. Rate constants and quantum yields of photolysis.** Dabigatran, rivaroxaban, and  
250 apixaban were irradiated under simulated solar light in unspiked and spiked purified water  
251 with nitrate ( $\text{NO}_3^-$ ) and hydrogen carbonate ( $\text{HCO}_3^-$ ) ions, in mineral and in river waters.  
252 Calculated rate constants, coefficients of determination, half-lives ( $t_{1/2}$ ), and polychromatic

253 quantum yields of photolysis are compiled in Table 1. In each case, NOACs photolysis  
254 followed apparent first-order kinetics. From dark control samples no thermal degradation and  
255 no hydrolysis were observed at the same time as the irradiation experiments.

256 Kinetics of photodegradation of dabigatran was dependent on the nature of the aqueous  
257 matrix. The calculated half-life was of 19.9 hours in deionized water and decreased by a  
258 factor of 2.7 to reach 7.4 hours in the mineral water. Afterwards, dabigatran was irradiated in  
259 purified water spiked with nitrate ions at a concentration of  $7.2 \text{ mg.L}^{-1}$  *i.e.*, the same  
260 concentration occurring in mineral water. The obtained half-life was of 6.8 hours, which is  
261 almost the same value as that obtained in mineral water. In river water (nitrate ions  
262 concentration:  $7.7 \text{ mg.L}^{-1}$ ), 50% of dabigatran was degraded in 24.1 hours; therefore, in this  
263 aqueous medium the degradation induced by light is less efficient by a factor 3.3 compared to  
264 the mineral water.

265 For rivaroxaban, kinetics of photodegradation were not significantly dependent on the nature  
266 of the aqueous matrix. In fact, half-lives of 2.3, 2.1, and 2.2 hours were obtained in purified,  
267 mineral, and river waters, respectively. Photolysis of rivaroxaban in purified water spiked  
268 with nitrate ions led to a half-life of 2.0 hours.

269 The behavior of apixaban under simulated solar light irradiation is a function of the aqueous  
270 medium. In purified water no degradation of the drug was observed after 19 hours of  
271 irradiation. At the opposite, in mineral water, a degradation was observed with a calculated  
272 half-life of 23.6 hours. This half-life decreased by a factor of 2.3 (10.4 hours) when apixaban  
273 was irradiated in purified water in the presence of nitrate ions. When both nitrate and  
274 hydrogen carbonate ( $74.0 \text{ mg.L}^{-1}$ ) ions were present in the medium, the half-life increased to  
275 26.9 hours. In the river water, 50% of degradation would be reached after 96.3 hours, clearly  
276 showing a lowering of the photodegradation efficiency.

277 **Please insert Table 1.**

278  
279 From these results, we can state that among the three NOACs, dabigatran and rivaroxaban are  
280 subject to direct photolysis under simulated sunlight irradiation, *i.e.*, degradation occurs in  
281 purified water. At the opposite, direct photodegradation of apixaban is not significant. In  
282 addition to direct photolysis, photosensitized reactions are clearly observed for dabigatran and  
283 apixaban. Ions naturally present in the mineral water can be at the origin of this processes.  
284 The photosensitizing potential of nitrate ions was particularly reviewed by Mack and Bolton  
285 (1999). These ions absorb solar light and then react with water to produce highly reactive  
286 hydroxyl radicals (Zuo et al., 2006; Chen et al., 2013). The photodegradation kinetics of  
287 dabigatran is accelerated in mineral water and in purified water spiked with nitrate ions. Both  
288 aqueous media led to a half-life close to 7.0 hours. We can thus conclude that the ion mainly  
289 responsible for the acceleration of dabigatran photodegradation was  $\text{NO}_3^-$ . In the case of  
290 apixaban, circumstances are slightly different. Nitrate ions are also proved to accelerate the  
291 drug photolysis but this result is not sufficient to explain the obtained half-life in mineral  
292 water. In fact, 50% of degradation would be reached after 23.6 and 10.4 hours in mineral  
293 water and deionized water spiked with  $\text{NO}_3^-$ , respectively. Addition of hydrogen carbonate  
294 ions to water spiked with nitrate ions induced an increase of the half-life by a factor of 2.6 ( $t_{1/2}$   
295 = 26.9 h). Hydrogen carbonate ions are among the most widespread anions in environmental  
296 waters and they are known to act as scavengers of hydroxyl radicals (Nakatani et al., 2007;  
297 Tercero Espinoza et al., 2007). Therefore, in our case the increase of apixaban half-life is  
298 mainly due to the reaction of  $\text{HCO}_3^-$  ions with hydroxyl radicals produced by nitrate ions  
299 under simulated sunlight irradiation. Finally, rivaroxaban photolysis seems not to be  
300 significantly impacted by ions present in the mineral water. This result can be explained by  
301 the very fast direct phototransformation of rivaroxaban. As a consequence, indirect  
302 photochemistry is unable to affect the phototransformation rate significantly.

303 In the river water, the concentration of nitrate ions ( $7.7 \text{ mg.L}^{-1}$ ) is close to that measured in  
304 mineral water ( $7.2 \text{ mg.L}^{-1}$ ). The concentration of hydrogen carbonate ions is included between  
305 200 and  $140 \text{ mg.L}^{-1}$ , *i.e.*, at least twice as high as in mineral water. Thus, the  $\text{HCO}_3^-$  ions  
306 scavenging effect is expected to be more efficient in river water than in mineral water. In  
307 surface waters, the ions effects are added to those of DOM that can act as photosensitizer, as  
308 screen through competitive light absorption, as inhibitor of triplet-sensitized transformation  
309 by reducing partially oxidized intermediates to the starting compounds, and as radical  
310 scavenger (Walse et al., 2004; Wenk et al., 2011, Chen et al., 2013; Liang et al., 2015; Zhang  
311 et al., 2016). In the case of dabigatran, the half-life in river water increases by a factor of 3.3  
312 in comparison with the mineral water. This increase cannot be assigned only to the  
313 scavenging effect of  $\text{HCO}_3^-$  ions. In fact, the comparison of results in mineral water and in  
314 purified water spiked with  $\text{NO}_3^-$  ions shows no clear effect of  $\text{HCO}_3^-$  ions on the rate constants  
315 for photolysis of dabigatran (Table 1). In the same way, apixaban half-life increases by a  
316 factor of 4.1. Thus, the increase of half-lives of dabigatran and apixaban cannot be explained  
317 only by the concentration increase of  $\text{HCO}_3^-$  ions in the river water but by the effect of DOM.  
318 Results obtained with rivaroxaban help to understand its role. In fact, rivaroxaban  
319 phototransformation is apparently not impacted by the presence of DOM. Thus, no significant  
320 screen effect is observed from DOM (see SF1 of supplementary materials). This result leads  
321 to the conclusion that the observed slowing down of the degradation of dabigatran and  
322 apixaban in river water is mainly due to a scavenging of hydroxyl radicals. The effect of  
323 DOM is emphasized with apixaban, for which the degradation occurs only by means of  
324 photosensitization.

325 Finally, the efficiency of NOACs direct photolysis was evaluated from polychromatic  
326 quantum yields of photodegradation. Values of  $2.2 \times 10^{-4}$  and  $4.4 \times 10^{-2} \text{ mol.E}^{-1}$  were calculated  
327 for dabigatran and rivaroxaban, respectively. Dabigatran absorbs sunlight to a higher extent

328 than rivaroxaban (Fig. 1), which partially offset the strong difference in the photolysis  
329 quantum yields. In the case of apixaban, no quantum yield for photolysis was determined due  
330 to the absence of degradation after 19 hours of simulated sunlight irradiation.

331

332 **3.3. Structures of NOACs photoproducts.** For each NOAC, non-irradiated and irradiated  
333 solutions were analyzed by means of LC-QToF-MS. Three products (D1, D2, and D3) were  
334 observed for dabigatran and one product (R1) for rivaroxaban, both irradiated in purified  
335 water. For apixaban, seven products (A1 to A7) were observed in mineral water. Results are  
336 gathered in Table 2.

337 In the case of dabigatran, among the three photoproducts observed two of them were  
338 associated to the drug photodegradation (Fig. 2). These compounds have  $m/z$  of 136.0874  
339 (D1,  $C_7H_{10}N_3$ ) and 323.1145 (D2,  $C_{17}H_{15}N_4O_3$ ). D1 fragmentation spectrum displays  $m/z$  at  
340 119 (-17) associated to the loss of a  $NH_3$  group located on the amidine part, and at 92 (-27)  
341 associated to the loss of the  $C=NH$  fragment (see SF4 of supplementary materials).

342

343

**Please insert Table 2.**

344

345 D1 was identified as the 4-aminobenzamidine (4-AB). This hypothesis was confirmed from  
346 LC-UV (Fig. 3a) and LC-QToF (see SF4 of supplementary materials) analyses of the  
347 standard. 4-AB is known to act as inhibitor of trypsin, an enzyme involved in the digestion of  
348 proteins (Safarik et al., 2002). D2 structure is formed from the other moiety of dabigatran for  
349 which an intramolecular cyclization and a demethylation occurred (Fig. 2). Only one fragment  
350 ( $m/z = 251$ ) is clearly observed for D2. This fragment is associated to a decarboxylation and a  
351 CO elimination. The UV spectrum of D2 is displayed in Fig. 3a.

352

**Please insert Fig. 2.**



353 Finally, a last photoproduct (D3) with a  $m/z$  of 279.1248 ( $C_{16}H_{15}N_4O$ ) was observed. This  
354 compound is not directly formed from dabigatran but from D2. In fact, D2 and D3 have a  $m/z$   
355 difference of 44 ( $CO_2$  group) and produce the same fragment at  $m/z = 251$ . Therefore, we can  
356 assume that D3 is formed from the photo-decarboxylation of D2.

357

358 **Please insert Fig. 3.**

359

360 Rivaroxaban degradation induced by simulated solar light irradiation in purified water  
361 produces only one main photoproduct with molecular ion at  $m/z$  436.0732 (named R1) in  
362 ESI+ mode (Table 2). R1 has the same  $m/z$  as rivaroxaban, *i.e.* a photoisomerization occurred.  
363 The UV absorption spectrum of R1 displays one band at 245 nm while that of rivaroxaban  
364 presents a maximum at 248 nm with a shoulder at 273 nm (Fig. 3b). The substituted thiophene  
365 moiety is responsible for the maximum of absorption around 245 nm (Boig et al., 1953); this  
366 part of the parent compound is unchanged in R1. This result is supported by the presence of a  
367 fragment at  $m/z$  145 assigned to the substituted thiophene ring and observed on both spectra  
368 of isomers (see SF8 of supplementary materials).

369

370 **Please insert Fig. 4.**

371

372 Processes of photoisomerization involving an intramolecular cyclisation as photo-Fries  
373 (Sandner et al., 1968) and Norrish type II reaction (Norrish et al., 1937) were considered. The  
374 two processes lead to structures in which the substituted thiophene ring is unchanged as  
375 validated using high field NMR. Indeed,  $^1H$  and  $^{13}C$  NMR spectra show the same splitting  
376 patterns for both compounds (see SF9 and SF10 of supplementary materials). The SOFAST-  
377 HMQC  $^1H$ - $^{15}N$  2D map undoubtedly shows the presence of a NH group in the R1 structure

378 (Fig. 4a) and the TOCSY sequence clearly exhibits two correlation pathways between NH  
379 proton (8.93 and 8.75 for R and R1 structures, respectively) and protons at 3.74 (J3), 4.92  
380 (J4), and 4.24/3.95 (J5) ppm for R, 4.24/3.95 (J5) ppm for R and 3.74/3.84 ppm (J3), 4.96  
381 (J4), and 4.00/4.26 (J5) ppm for R1 (Fig. 4b). On this basis, the proposed structure for R1 is  
382 presented in Fig. 5.

383

384

**Please insert Fig. 5.**

385

386 The simulated sunlight irradiation of apixaban in mineral water results in the clear observation  
387 of seven photoproducts (Table 2). Assuming that LC-MS/MS structure responses are the same  
388 for each compound, four degradation products can be considered as major (A3, A5, A6, and  
389 A7). Their structures are presented in Fig. 6. Structures of minor photoproducts have also  
390 been determined (A1, A2, and A4; see SS2, SS3, and SS5 of supplementary materials).

391

392

**Please insert Fig. 6.**

393

394 A1 ( $m/z = 191.1186$ ) and A2 ( $m/z = 287.1146$ ) are assigned to  $C_{11}H_{15}N_2O$  and  $C_{14}H_{15}N_4O_3$ ,  
395 chemical formula, respectively. Concerning the main photoproducts, A3 (354.1581,  
396  $C_{18}H_{20}N_5O_3$ ) is formed from the release of methoxybenzene, A4 and A5 (476.1939,  
397  $C_{25}H_{26}N_5O_5$ ) are obtained by hydroxylation of the phenyl group, A6 (446.1818,  $C_{24}H_{24}N_5O_4$ )  
398 is formed from the substitution of the methoxy group by a hydroxy group, and A7 (458.1820,  
399  $C_{25}H_{24}N_5O_4$ ) is obtained from the formation of an unsaturation into the 2-oxo-1-piperidinyl  
400 ring linked to the pyrazole ring. This latter structure is in agreement with a polarity lowering  
401 and thus a retention time increase. The fragmentation pattern of each photoproduct is  
402 described in SS4, SS6, SS7, and SS8 of supplementary materials.

#### 403 **4. Conclusion**

404 Kinetics of photodegradation show that photolysis can be one of the main ways of  
405 degradation for NOACs present in surface waters. Rivaroxaban degradation is not  
406 significantly impacted by the nature of the aqueous matrix. This compound seems only to  
407 undergo direct photolysis leading to a photoisomerization. The structure of the photoisomer  
408 has been clearly identified from NMR spectra. Dabigatran is photolyzed by direct and indirect  
409 routes. Nitrate ions are mainly responsible for the acceleration of dabigatran degradation.  
410 Results in river water show that dissolved organic matter slows down the degradation of  
411 dabigatran probably related to its action as a scavenger of hydroxyl radicals. Two  
412 photoproducts are formed, *i.e.* the 4-aminobenzamidine and a cyclization product. Apixaban  
413 is degraded only by photosensitization which is induced by nitrate ions. At the opposite,  
414 hydrogen carbonate ions partially block the degradation of apixaban. This effect is also  
415 observed in the presence of dissolved organic matter. Seven photoproducts were clearly  
416 identified under simulated solar light irradiation of apixaban.  
417 Following these results, it will be important to evaluate the ecotoxicological impact of  
418 NOACs photoproducts. Compounds of potential concern are especially the isomer of  
419 rivaroxaban and the 4-aminobenzamidine, which is a known inhibitor of trypsin and could be  
420 at the origin of toxic effects.

421

#### 422 **ACKNOWLEDGEMENTS**

423 This work was supported by the French national program EC2CO-Ecodyn (PATNACOT).  
424 Financial support from the TGIR-RMN-THC Fr3050 CNRS for conducting the research is  
425 gratefully acknowledged. The authors also would to thank the multidisciplinary Seine Aval  
426 scientific program (CRAPPSE project), sponsored by the GIP Seine-Aval ([http://seine-  
427 aval.crihan.fr/web/](http://seine-aval.crihan.fr/web/)). This study has been carried out in the frame of the Investments for the

428 future Programme, within the Cluster of Excellence COTE (ANR-10-LABX 45). EPOC UMR  
429 (5805) is gratefully acknowledged for the financial support (“projets innovants”) of a part of  
430 this study.

431

#### 432 **SUPPLEMENTARY MATERIALS**

433 Supplementary information related to this article can be found at

ACCEPTED MANUSCRIPT

434 **REFERENCES**

- 435 ACD software, calculated using Advanced Chemistry Development (ACD/Labs) Software  
436 V11.02 (© 1994-2016 ACD/Labs).
- 437 ANSM, 2013. Evolution des ventes des anticoagulants oraux en France de janvier 2008 à  
438 septembre 2013. [http://ansm.sante.fr/Dossiers/Les-anticoagulants/Quelle-est-la-](http://ansm.sante.fr/Dossiers/Les-anticoagulants/Quelle-est-la-situation-actuelle-de-l-utilisation-des-NACO/(offset)/1)  
439 [situation-actuelle-de-l-utilisation-des-NACO/\(offset\)/1](http://ansm.sante.fr/Dossiers/Les-anticoagulants/Quelle-est-la-situation-actuelle-de-l-utilisation-des-NACO/(offset)/1). January 27th, 2017.
- 440 Beyer-Westendorf, J., Gelbricht, V., Förster, K., Ebertz, F., Röllig, D., Schreier, T., Tittl, L.,  
441 Thieme, C., Hänsel, U., Köhler, C., Werth, S., Kuhlisch, E., Stange, T., Röder, I.,  
442 Weiss, N., 2014. Safety of switching from vitamin K antagonists to dabigatran or  
443 rivaroxaban in daily care--results from the Dresden NOAC registry. *Br. J. Clin.*  
444 *Pharmacol.* 78 (4), 908-17.
- 445 Boig, F.S., Costa, G.W., Osvar, I., 1953. Ultraviolet Absorption Spectra in the Thiophene  
446 Series. Halogen and Nitro Derivatives. *J. Org. Chem.* 18 (7), 775-778.
- 447 Carlson, J.C., Stefan, M.I., Parnis, J.M., Metcalfe, C.D., 2015. Direct UV photolysis of  
448 selected pharmaceuticals, personal care products and endocrine disruptors in aqueous  
449 solution. *Water Res.* 84, 350-361.
- 450 Chen, Y., Zhang, K., Zuo, Y., 2013. Direct and indirect photodegradation of estriol in the  
451 presence of humic acid, nitrate and iron complexes in water solutions. *Sci. Total*  
452 *Environ.* 463-464, 802-809.
- 453 Chen, Y., Liu, L., Su, J., Liang, J., Wu, B., Zuo, J., Zuo, Y., 2017. Role of humic substances  
454 in the photodegradation of naproxen under simulated sunlight. *Chemosphere.* 187,  
455 261-267.
- 456 El-Helou, N., Al-Hajje, A., Ajrouche, R., Awada, S., Rachidi, S., Zein, S., Salameh, P., 2013.  
457 Adverse drug events associated with vitamin K antagonists: factors of therapeutic  
458 imbalance. *Vasc. Health Risk Manag.* 9, 81-8.

- 459 eVidal, data bank [on line], [www.eVidal.fr](http://www.eVidal.fr). January 27<sup>th</sup>, 2017.
- 460 Frost, C., Wang, J., Nepal, S., Schuster, A., Barrett, Y.C., Mosqueda-Garcia, R., Reeves,  
461 R.A., LaCreta, F., 2013. Apixaban, an oral, direct factor Xa inhibitor: single dose  
462 safety, pharmacokinetics, pharmacodynamics and food effect in healthy subjects. *Br.*  
463 *J. Clin. Pharmacol.* 75 (2), 476-87.
- 464 Gulseth, M.P., Michaud, J., Nutescu, E.A., 2008. Rivaroxaban: an oral direct inhibitor of  
465 factor Xa. *Am. J. Health Syst. Pharm.* 15, 65 (16), 1520-9.
- 466 Hanslik, T., Prinseau, J., 2004. The use of vitamin K in patients on anticoagulant therapy: a  
467 practical guide. *Am. J. Cardiovasc. Drug.* 4 (1), 43-55.
- 468 Kasad, P.A., 2013. Photolytic-Thermal Degradation Study And Method Development Of  
469 Rivaroxaban By RP-HPLC. *Int. J. Pharm. Tech. Res.* 5 (3), 1254.
- 470 Khoo, C.W., Lip, G.Y., 2010. Insights from the dabigatran versus warfarin in patients with  
471 atrial fibrillation (RE-LY) trial. *Expert. Opin. Pharmacother.* 11 (4), 685-7.
- 472 Liang, C., Zhao, H., Deng, M., Quan, X., Chen, S., Wang, H., 2015. Impact of dissolved  
473 organic matter on the photolysis of the ionizable antibiotic norfloxacin. *J. Environ.*  
474 *Sci.* 27, 115-123.
- 475 Mack, J., Bolton, R.B., 1999. Photochemistry of nitrite and nitrate in aqueous solution: a  
476 review. *J. Photochem. Photobiol. A.* 128, 1-13.
- 477 Nakatani, N., Hashimoto, N., Shindo, H., Yamamoto, M., Kikkawa, M., Sakugawa, H., 2007.  
478 Determination of photoformation rates and scavenging rate constants of hydroxyl  
479 radicals in natural waters using an automatic light irradiation and injection system.  
480 *Anal. Chim. Acta.* 581, 260-267.
- 481 Norrish, R.G.W., Bamford, C.H., 1937. Photo-decomposition of Aldehydes and Ketones.  
482 *Nature.* 140, 195-196.

- 483 Pollack, C.V., Reilly, P.A., Eikelboom, J., Glund, S., Verhamme, P., Bernstein, R.A., Dubiel,  
484 R., Huisman, M.V., Hylek, E.M., Kamphuisen, P.W., Kreuzer, J., Levy, J.H., Sellke,  
485 F.W., Stangier, J., Steiner, T., Wang, B., Kam, C-W., Weitz, J.I., 2015. Idarucizumab  
486 for Dabigatran Reversal. *N. Engl. J. Med.* 373, 511-520.
- 487 Ramiseti, N.R., Kuntamukkala, R., 2014. Development and validation of a stability  
488 indicating LC-PDA-MS/MS method for separation, identification and characterization  
489 of process related and stress degradation products of rivaroxaban. *RSC Adv.* 4, 23155.
- 490 Safarik, I., Ptackova, L., Koneracka, M., Safarikova, M., Timko, M., Kopcansky, P., 2002.  
491 Determination of selected xenobiotics with ferrofluid-modified trypsin. *Biotechnol.*  
492 *Lett.* 24, 355-358.
- 493 Sandner, M.R., Hedaya, E., Trecker, D.J., 1968. Mechanistic Studies of the Photo-Fries  
494 Reaction. *J. Am. Chem. Soc.* 90 (26), 7249-7254.
- 495 Secrétan, P.-H., Sadou-Yayé, H., Aymes-Chodur, C., Bernard, M., Solgadi, A., Amrani, F.,  
496 Yagoubia, N., Do, B., 2015. A comprehensive study of apixaban's degradation  
497 pathways under stress conditions using liquid chromatography coupled to multistage  
498 mass spectrometry. *RCS Adv.* 5, 35586.
- 499 Siegal, D.M., Curnutte, J.T., Connolly, S.J., Lu, G., Conley, P.B., Wiens, B.L., Mathur, V.S.,  
500 Castillo, J., Bronson, M.D., Leeds, J.M., Mar, F.A., Gold, A., Crowther, M.A., 2015.  
501 Andexanet Alfa for the Reversal of Factor Xa Inhibitor Activity. *N. Engl. J. Med.* 373,  
502 2413-2424.
- 503 Spyropoulos, A.C., 2008. Brave new world: the current and future use of novel  
504 anticoagulants. *Thromb. Res.* 123, 29-35.
- 505 Swain, D., Patel, P.N., Nagaraj, G., Srinivas, K.S., Sharma, M., Garg, P., Samanthula, G.,  
506 2016. Liquid Chromatographic Method Development for Forced Degradation Products

- 507 of Dabigatran Etexilate: Characterisation and In Silico Toxicity Evaluation.  
508 *Chromatographia*. 79, 169-178.
- 509 Szabo, R.K., Megyeri, Cs., Illes, E., Gajda-Schranz, K., Mazellier, P., Dombi, A., 2011.  
510 Phototransformation of ibuprofen and ketoprofen in aqueous solutions. *Chemosphere*.  
511 84 (11), 1658-1663.
- 512 Tantawy, M.A., El-Ragehy, N.A., Hassan, N.Y., Abdelkawy, M., 2016. Stability-indicating  
513 spectrophotometric methods for determination of the anticoagulant drug apixaban in  
514 the presence of its hydrolytic degradation product. *Spectrochim. Acta A*. 159, 13-20.
- 515 Tercero Espinoza, L.A., Neamtu, M., Frimmel, F.H., 2007. The effect of nitrate, Fe(III) and  
516 bicarbonate on the degradation of bisphenol A by simulated solar UV-irradiation.  
517 *Water Res.* 41, 4479-4487.
- 518 Walse, S.S., Morgan, S.L., Kong, L., Ferry, J.L., 2004. Role of Dissolved Organic Matter,  
519 Nitrate, and Bicarbonate in the Photolysis of Aqueous Fipronil. *Environ. Sci. Technol.*  
520 38 (14), 3908–3915.
- 521 Wanat, M.A., 2013. Novel oral anticoagulants: a review of new agents. *Postgrad. Med.* 125  
522 (4), 103-14.
- 523 Wenk, J., von Gunten, U., Canonica, S., 2011. Effect of Dissolved Organic Matter on the  
524 Transformation of Contaminants Induced by Excited Triplet States and the Hydroxyl  
525 Radical. *Environ. Sci. Technol.* 45 (4), 1334-1340.
- 526 Wingert, N.R., dos Santosa, N.O., Nunes, M.A.G., Gomes, P., Müller, E. I., Flores, E.M.M.,  
527 Steppe, M., 2016. Characterization of three main degradation products from novel oral  
528 anticoagulant rivaroxaban under stress conditions by UPLC-Q-TOF-MS/MS. *J.*  
529 *Pharmaceut. Biomed.* 123, 10-15.
- 530 Zhang, R., Yang, Y., Huang, C.H., Li, N., Liu, H., Zhao, L., Sun, P., 2016. UV/H<sub>2</sub>O<sub>2</sub> and  
531 UV/PDS Treatment of Trimethoprim and Sulfamethoxazole in Synthetic Human



- 532 Urine: Transformation Products and Toxicity. *Environ. Sci. Technol.* 50 (5), 2573-  
533 2583.
- 534 Zhang, Y.-N., Xie, Q., Sun, G., Yang, K., Song, S., Chen, J., Zhou, C., Li, Y., 2016. Effects  
535 of dissolved organic matter on phototransformation rates and dioxin products of  
536 triclosan and 2'-HO-BDE-28 in estuarine water. *Environ. Sci.: Processes Impacts*.  
537 DOI: 10.1039/C6EM00122J.
- 538 Zuo, Y., Wang, C., Van, T., 2006. Simultaneous determination of nitrite and nitrate in dew,  
539 rain, snow and lake water samples by ion-pair high-performance liquid  
540 chromatography. *Talanta*. 70, 281-285.
- 541 Zuo, Y., Zhang, K., Zhou, S., 2013. Determination of estrogenic steroids and microbial and  
542 photochemical degradation of 17  $\alpha$ -ethinylestradiol (EE2) in lake surface water, a case  
543 study. *Environ. Sci. Process. Impacts*. 15(8), 1529-1535.
- 544 Zuo, Y., 2014. *High-Performance Liquid Chromatography (HPLC): Principles, Procedures*  
545 *and Practices*. Nova Science Publishers, Inc., UK ed. edition, New York.

1 Photodegradation of novel oral anticoagulants under sunlight irradiation in  
2 aqueous matrices

3  
4 Montaha Yassine<sup>1ab,2</sup>, Laura Fuster<sup>1ab</sup>, Marie-Hélène Dévier<sup>1ab</sup>, Emmanuel Geneste<sup>1ab</sup>, Patrick  
5 Pardon<sup>1ab</sup>, Axelle Grélard<sup>3</sup>, Erick Dufourc<sup>3</sup>, Mohamad Al Iskandarani<sup>2</sup>, Selim Aït-Aïssa<sup>4</sup>,  
6 Jeanne Garric<sup>5</sup>, Hélène Budzinski<sup>1ab</sup>, Patrick Mazellier<sup>1ab</sup>, Aurélien S. Trivella<sup>1ab,\*</sup>

7  
8 <sup>1a</sup>Univ. Bordeaux, UMR EPOC CNRS 5805, LPTC, F-33405 Talence, France

9 <sup>1b</sup>CNRS, EPOC, UMR 5805, LPTC, F-33400 Talence, France

10 <sup>2</sup>National Council of Scientific Research (NCSR), Lebanese Atomic Energy Commission  
11 (LAEC), Laboratory of Analysis of Organic Pollutants (LAOP), B. P. 11-8281, Riad El Solh -  
12 1107 2260 - Beirut, Lebanon

13 <sup>3</sup>Institute of Chemistry and Biology of Membranes and Nano-objects, CBMN UMR 5248,  
14 CNRS University of Bordeaux, Bordeaux National Institute of Technology, Allée Geoffroy St  
15 Hilaire, Pessac, France

16 <sup>4</sup>INERIS, Unité d'écotoxicologie *in vitro* et *in vivo* (ECOT), Verneuil-en-Halatte, France

17 <sup>5</sup>Irstea, UR MALY, centre de Lyon-Villeurbanne, F-69616 Villeurbanne, France

18  
19  
20 \*Corresponding author: Aurélien Trivella

21 [aurelien.trivella@u-bordeaux.fr](mailto:aurelien.trivella@u-bordeaux.fr)

22 Tel: +33 (0)553352429

23

24

25

26

27

## Tables

28  
29  
30  
31  
32  
33  
34  
35

**Table 1**

Apparent first-order rate constants ( $k$ ,  $\text{min}^{-1}$ ), coefficients of determination ( $R^2$ ), half-lives ( $t_{1/2}$ , h), and polychromatic quantum yields of photolysis ( $\phi$ ,  $\text{mol}\cdot\text{E}^{-1}$ ) obtained from Suntest irradiation of NOACs in aqueous matrices. ND: not degraded. Error bar on first-order rate constants:  $\pm 10\%$ .

NOAC	Aqueous matrix	$k \times 10^4$	$R^2$	$t_{1/2}$	$\phi$
Dabigatran	purified water	6.0	0.9944	19.9	$2.2 \times 10^{-4}$
	mineral water	14.1	0.9778	7.4	-
	purified water + $\text{NO}_3^-$	17.1	0.9953	6.8	-
	river water	4.7	0.9633	24.1	-
Rivaroxaban	purified water	49.4	0.9975	2.3	$4.4 \times 10^{-2}$
	mineral water	55.9	0.9943	2.1	-
	purified water + $\text{NO}_3^-$	57.5	0.9808	2.0	-
	river water	51.6	0.9960	2.2	-
Apixaban	purified water	ND	-	-	ND
	mineral water	4.9	0.9924	23.6	-
	purified water + $\text{NO}_3^-$	11.1	0.9892	10.4	-
	purified water + $\text{NO}_3^-$ + $\text{HCO}_3^-$	4.3	0.9823	26.9	-
	river water	1.2	0.9875	96.3	-

36  
37

38

39 **Table 2**

40 LC-MS/MS (ESI+) analyses of NOACs and of their photoproducts. RT: retention time.

NOAC	Name	m/z (RT in min)	Proposed chemical formula	$\Delta(m/z)$ (ppm)	Fragments (relative intensity in %)
Dabigatran	D	472.2116 (2.2)	$C_{25}H_{26}N_7O_3$	-4.02	-
	D1	136.0874 (1.0)	$C_7H_{10}N_3$	0.73	119 (100), 92 (17)
	D2	323.1145 (2.3)	$C_{17}H_{15}N_4O_3$	-0.31	251 (100)
	D3	279.1248 (3.2)	$C_{16}H_{15}N_4O$	-0.72	251 (100)
Rivaroxaban	R	436.0739 (11.3)	$C_{19}H_{19}ClN_3O_5S$	-1.15	-
	R1	436.0732 (8.2)	$C_{19}H_{19}ClN_3O_5S$	0.46	436 (73), 231 (63), 145 (100)
Apixaban	A	460.2012 (11.7)	$C_{25}H_{26}N_5O_4$	-5.87	-
	A1	191.1186 (1.5)	$C_{11}H_{15}N_2O$	-1.05	191 (100), 147 (16), 107 (13)
	A2	287.1146 (5.3)	$C_{14}H_{15}N_4O_3$	-0.70	270 (100), 242 (9)
	A3	354.1581 (5.5)	$C_{18}H_{20}N_5O_3$	-4.24	337 (100)
	A4	476.1939 (8.0)	$C_{25}H_{26}N_5O_5$	-1.05	459 (100), 241 (13), 199 (74)
	A5	476.1939 (8.5)	$C_{25}H_{26}N_5O_5$	-1.05	459 (100), 361 (11), 241 (18), 200 (13), 199 (70)
	A6	446.1818 (8.8)	$C_{24}H_{24}N_5O_4$	2.24	430 (23), 429 (83), 282 (13), 227 (15), 186 (13), 185 (100), 171 (12), 93 (11)
	A7	458.1820 (12.3)	$C_{25}H_{24}N_5O_4$	1.75	458 (42), 441 (100), 385 (64), 342 (10), 277 (15), 199 (36)

41

1 Photodegradation of novel oral anticoagulants under sunlight irradiation in  
2 aqueous matrices

3  
4 Montaha Yassine<sup>1ab,2</sup>, Laura Fuster<sup>1ab</sup>, Marie-Hélène Dévier<sup>1ab</sup>, Emmanuel Geneste<sup>1ab</sup>, Patrick  
5 Pardon<sup>1ab</sup>, Axelle Grélard<sup>3</sup>, Erick Dufourc<sup>3</sup>, Mohamad Al Iskandarani<sup>2</sup>, Selim Aït-Aïssa<sup>4</sup>,  
6 Jeanne Garric<sup>5</sup>, Hélène Budzinski<sup>1ab</sup>, Patrick Mazellier<sup>1ab</sup>, Aurélien S. Trivella<sup>1ab,\*</sup>

7  
8 <sup>1a</sup>Univ. Bordeaux, UMR EPOC CNRS 5805, LPTC, F-33405 Talence, France

9 <sup>1b</sup>CNRS, EPOC, UMR 5805, LPTC, F-33400 Talence, France

10 <sup>2</sup>National Council of Scientific Research (NCSR), Lebanese Atomic Energy Commission  
11 (LAEC), Laboratory of Analysis of Organic Pollutants (LAOP), B. P. 11-8281, Riad El Solh -  
12 1107 2260 - Beirut, Lebanon

13 <sup>3</sup>Institute of Chemistry and Biology of Membranes and Nano-objects, CBMN UMR 5248,  
14 CNRS University of Bordeaux, Bordeaux National Institute of Technology, Allée Geoffroy St  
15 Hilaire, Pessac, France

16 <sup>4</sup>INERIS, Unité d'écotoxicologie *in vitro* et *in vivo* (ECOT), Verneuil-en-Halatte, France

17 <sup>5</sup>Irstea, UR MALY, centre de Lyon-Villeurbanne, F-69616 Villeurbanne, France

18  
19  
20 \*Corresponding author: Aurélien Trivella

21 [aurelien.trivella@u-bordeaux.fr](mailto:aurelien.trivella@u-bordeaux.fr)

22 Tel: +33 (0)553352429

23

24

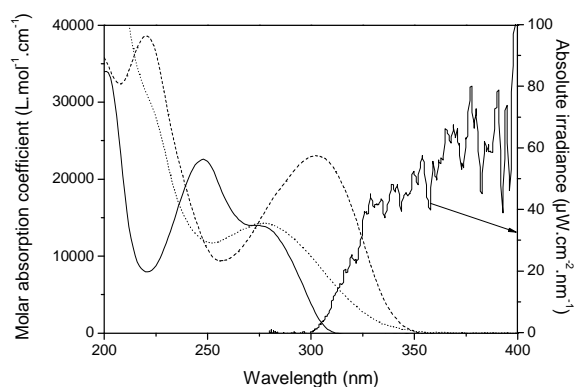
25

26

27

## Figures

28  
29  
30



31

32 **Fig. 1.** UV absorption spectra of dabigatran (dashed line) and rivaroxaban (solid line)

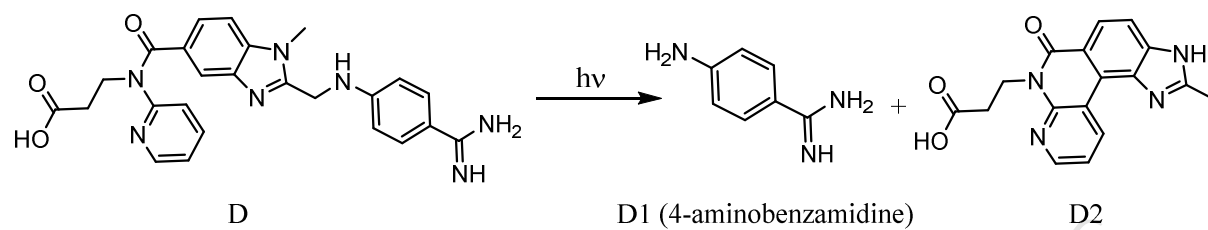
33 dissolved in purified water, and of apixaban (dotted line) dissolved in a methanol-water

34 mixture. Solar light emission spectrum at the Earth surface on May 5, 2016 at coordinates

35 (45.195510, 0.718811).

36

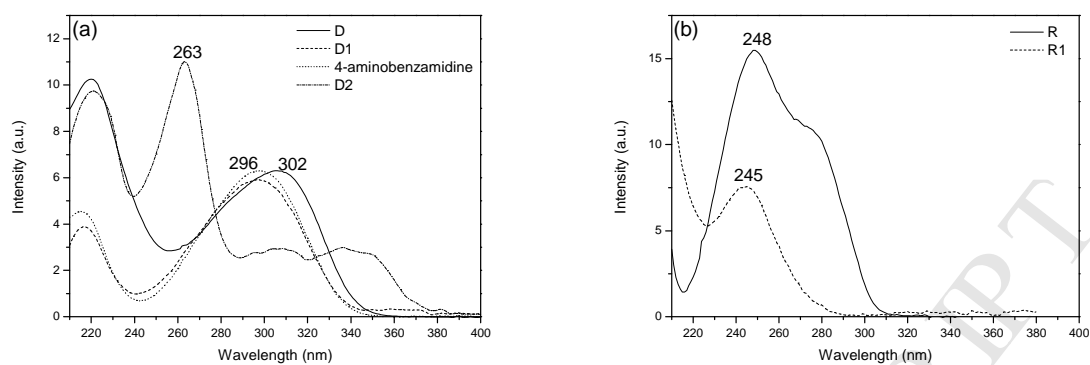
37

38  
3940 **Fig. 2.** Photodegradation of dabigatran under simulated solar light irradiation in purified

41 water.

42

43



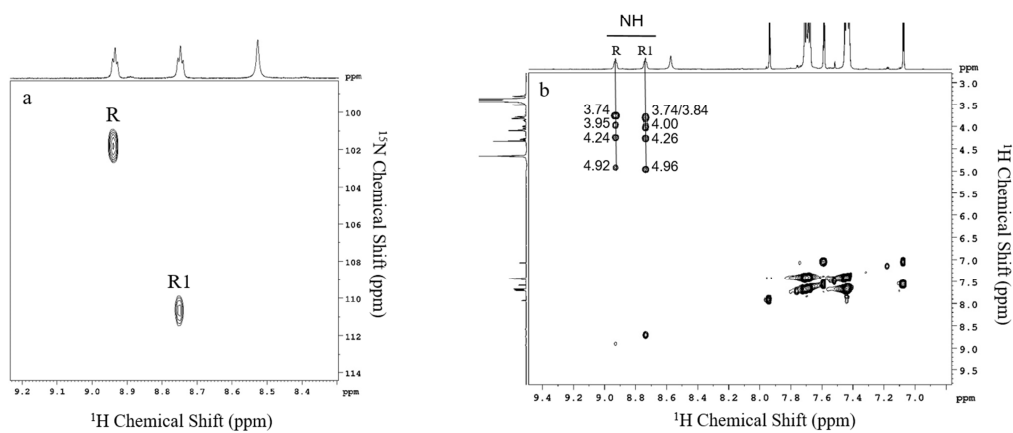
44

45 **Fig. 3.** UV absorption spectra of (a) dabigatran (solid line), D1 (dashed line), 4-  
46 aminobenzamidine (dotted line), and D2 (dashed-dotted line); (b) rivaroxaban (solid line) and  
47 of its photoisomer (R1, dashed line).

48



49

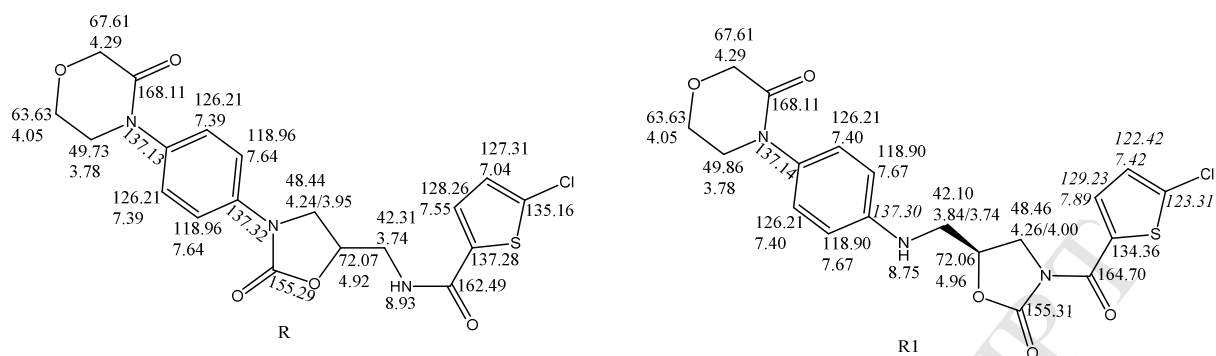


50

51 **Fig. 4.** Selected expansions of 2D NMR spectra of rivaroxaban (R) and of its photoisomer  
52 (R1) in MeOH- $\text{d}_3$ : (a) SOFAST-HMQC  $^1\text{H}$ - $^{15}\text{N}$  and (b) TOCSY NMR spectra.

53

54



55

56

57 **Fig. 5.** <sup>13</sup>C and <sup>1</sup>H chemical shifts (ppm) of rivaroxaban (R) and its photoisomer (R1).

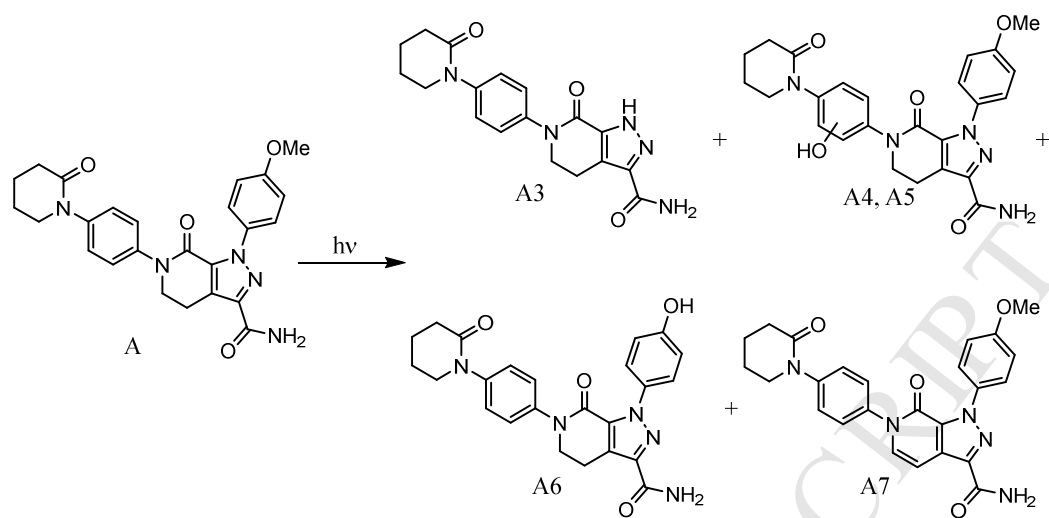
58 Chemical shifts in italics: the similarity of the two structures (R and R1) as well as the low

59 concentration of the samples did not allow, despite the use of a very high magnetic field, to

60 remove the ambiguity on the assignment of chemical shifts.

61

62



63

64 **Fig. 6.** Major photoproducts of apixaban formed under simulated solar light irradiation in  
65 mineral water.

66

67

Photodegradation of novel oral anticoagulants under sunlight irradiation in  
aqueous matrices

Montaha Yassine<sup>1ab,2</sup>, Laura Fuster<sup>1ab</sup>, Marie-Hélène Dévier<sup>1ab</sup>, Emmanuel Geneste<sup>1ab</sup>, Patrick Pardon<sup>1ab</sup>, Axelle Grélard<sup>3</sup>, Erick Dufourc<sup>3</sup>, Mohamad Al Iskandarani<sup>2</sup>, Selim Aït-Aïssa<sup>4</sup>, Jeanne Garric<sup>5</sup>, Hélène Budzinski<sup>1ab</sup>, Patrick Mazellier<sup>1ab</sup>, Aurélien S. Trivella<sup>1ab,\*</sup>

<sup>1a</sup>Univ. Bordeaux, UMR EPOC CNRS 5805, LPTC, F-33405 Talence, France

<sup>1b</sup>CNRS, EPOC, UMR 5805, LPTC, F-33400 Talence, France

<sup>2</sup>National Council of Scientific Research (NCSR), Lebanese Atomic Energy Commission (LAEC), Laboratory of Analysis of Organic Pollutants (LAOP), B. P. 11-8281, Riad El Solh - 1107 2260 - Beirut, Lebanon

<sup>3</sup>Institute of Chemistry and Biology of Membranes and Nano-objects, CBMN UMR 5248, CNRS University of Bordeaux, Bordeaux National Institute of Technology, Allée Geoffroy St Hilaire, Pessac, France

<sup>4</sup>INERIS, Unité d'écotoxicologie *in vitro* et *in vivo* (ECOT), Verneuil-en-Halatte, France

<sup>5</sup>Irstea, UR MALY, centre de Lyon-Villeurbanne, F-69616 Villeurbanne, France

\*Corresponding author: Aurélien Trivella

[aurelien.trivella@u-bordeaux.fr](mailto:aurelien.trivella@u-bordeaux.fr)

Tel: +33 (0)553352429

## Highlights

- Dabigatran undergoes direct and indirect photolysis,  $t_{1/2}$  is of 24h in river water.
- Direct photolysis is predominant for rivaroxaban,  $t_{1/2}$  is of 2.2h in river water.
- Argatroban is mainly photodegraded by photosensitization.
- Structures of main photoproducts have been identified.